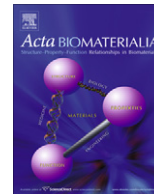




Contents lists available at ScienceDirect

Acta Biomaterialia

journal homepage: [www.elsevier.com/locate/actabiomat](http://www.elsevier.com/locate/actabiomat)

## Measurement of layer-specific mechanical properties in multilayered biomaterials by micropipette aspiration

Ruogang Zhao<sup>a,1</sup>, Krista L. Sider<sup>a,1</sup>, Craig A. Simmons<sup>a,b,c,\*</sup>

<sup>a</sup> Institute of Biomaterials and Biomedical Engineering, University of Toronto, 164 College Street, Toronto, Ontario, Canada M5S 3G9

<sup>b</sup> Department of Mechanical and Industrial Engineering, University of Toronto, 5 King's College Road, Toronto, Ontario, Canada M5S 3G8

<sup>c</sup> Faculty of Dentistry, University of Toronto, 124 Edward Street, Toronto, Ontario, Canada M5G 1G6

### ARTICLE INFO

#### Article history:

Received 29 July 2010

Received in revised form 12 October 2010

Accepted 2 November 2010

Available online xxx

#### Keywords:

Micropipette aspiration

Finite-element analysis

Micromechanical testing

Layered biomaterials

Heart valve

### ABSTRACT

Many biomaterials and tissues are complex multilayered structures in which the individual layers have distinct mechanical properties that influence the mechanical behavior and define the local cellular micro-environment. Characterization of the mechanical properties of individual layers in intact tissues is technically challenging. Micropipette aspiration (MA) is a proven method for the analysis of local mechanical properties of soft single-layer biomaterials, but its applicability for multilayer structures has not been demonstrated. We sought to determine and validate MA experimental parameters that would permit measurement of the mechanical properties of only the top layer of an intact multilayer biomaterial or tissue. To do so, we performed parametric nonlinear finite-element (FE) analyses and validation experiments using a multilayer gelatin system. The parametric FE analyses demonstrated that measurement of the properties of only the top layer of a multilayer structure is sensitive to the ratio of the pipette inner diameter ( $D$ ) to top layer thickness ( $t_{\text{top}}$ ), and that accurate measurement of the top layer modulus requires  $D/t_{\text{top}} < 1$ . These predictions were confirmed experimentally by MA of the gelatin system. Using this approach and an inverse FE method, the mean effective modulus of the fibrosa layer of intact porcine aortic valve leaflets was determined to be greater than that of the ventricularis layer ( $P < 0.01$ ), consistent with data obtained by tensile testing of dissected layers. This study provides practical guidelines for the use of MA to measure the mechanical properties of single layers in intact multilayer biomaterials and tissues.

© 2010 Acta Materialia Inc. Published by Elsevier Ltd. All rights reserved.

### 1. Introduction

Biomaterials and soft tissues, including skin [1], articular cartilage [2], heart valves [3] and vascular tissue [4], are often complex multilayered structures in which the individual layers have distinct mechanical properties that influence the overall mechanical behavior and define the local cellular microenvironment. The local heterogeneity in mechanical properties that can occur in these tissues, and in the biomaterials that mimic them, require microscale measurement techniques for mechanical characterization. Nano/microscale techniques such as nano/microindentation and atomic force microscopy (AFM) have often been employed to good effect to measure local mechanical properties of tissues and biomaterials [5–9]. However, these methods are technically complex, require specialized equipment, and, in the case of nanoindentation and

AFM, are limited to measuring properties within nanometers to a couple of microns of the test surface. While this is appropriate for measuring the properties of a thin surface layer or the cells lining a material (e.g. the endothelial layer on cardiovascular tissues), these methods cannot be used to measure the bulk properties of thicker (i.e.  $>10 \mu\text{m}$ ) biomaterial or tissue layers that define macroscopic mechanical behavior and the mechanical environment of embedded cells.

Micropipette aspiration (MA) has been widely used to measure the bulk mechanical properties of adherent or non-adherent biomaterials [10–18]. In this relatively simple and accessible technique, a local region of the tissue or biomaterial is aspirated into a small diameter glass pipette, and the aspiration length is measured as a function of the applied pressure. The apparent mechanical properties of the material are then estimated from the pressure–aspiration length curves using analytical models [2,13], numerically derived models [12] or inverse finite-element (FE) approaches [19]. However, the apparent mechanical properties measured by MA are sensitive to several experimental parameters, including the thickness of the material layer being measured, the pipette diameter and whether the sample is adhered to an

\* Corresponding author at: Department of Mechanical and Industrial Engineering, University of Toronto, 5 King's College Road, Toronto, Ontario, Canada M5S 3G8. Tel.: +1 416 946 0548; fax: +1 416 978 7753.

E-mail address: [c.simmons@utoronto.ca](mailto:c.simmons@utoronto.ca) (C.A. Simmons).

<sup>1</sup> These authors contributed equally to this work.

underlying substrate. Aoki et al. [13] used an FE model of a linear elastic material layer adhered to an underlying linear elastic substrate to determine that the underlying substrate has negligible influence on the apparent elastic modulus of the sample only when the ratio of the pipette inner diameter ( $D$ ) to the material layer thickness ( $t$ ) is less than 1 (i.e.  $D/t < 1$ ). An analytical model developed by Alexopoulos et al. [2] produced similar results to those of Aoki et al. for stiff top layers and small  $D/t$  ratios, but deviated significantly for soft top layers and large  $D/t$ . The discrepancy was attributed to the thickness of the underlying substrate, which was finite and fixed in the Aoki study but semi-infinite in the Alexopoulos model. Boudou et al. [12] used FE analysis to derive expressions for the elastic modulus of thin linear elastic single-layer biomaterials that account for the layer thickness and whether or not the layer is adhered to a rigid underlying substrate.

Collectively these computational studies suggest guidelines for the measurement of the modulus of the top layer of a multilayered linear elastic material. However, these studies did not consider the nonlinear material behavior that is common in most biomaterials and tissues [20] and have not been validated experimentally. Thus, the objective of the current study was to extend the previous studies to define the MA experimental parameters needed to measure the mechanical properties of only the top layer of an intact multilayer biomaterial or tissue. We hypothesized that this could be accomplished by appropriate selection of the pipette diameter. To test this hypothesis and define the appropriate diameter, we performed parametric nonlinear FE analyses and validation experiments on a dual-layer gelatin model system, testing the sensitivity of the measured modulus to the  $D/t$  ratio, and the thicknesses and elastic properties of the two layers. Finally, the validated experimental parameters were applied to estimate the effective moduli of individual layers of intact aortic valves.

## 2. Materials and methods

### 2.1. Finite element model of a dual-layer gel

An FE model of a dual-layer gel, representing a generic layered tissue or biomaterial, was developed (Fig. 1). A large deformation nonlinear hyperelastic FE model was used to account for nonlinearities that arise from large deformation, contact sliding between the gel and the micropipette wall, and material nonlinearity. The

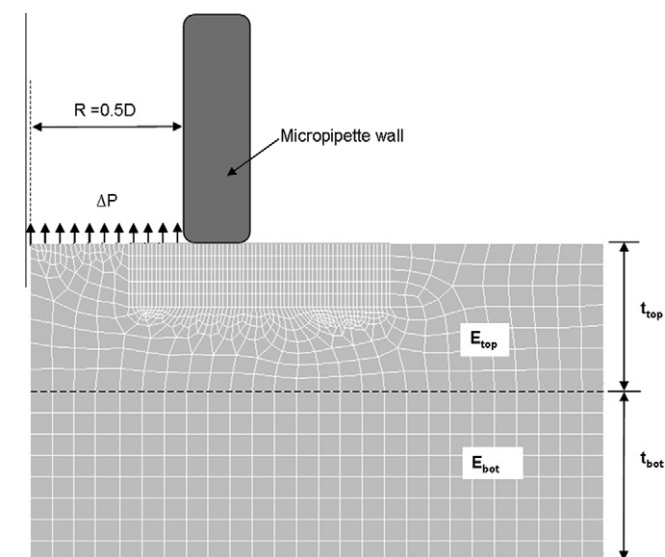


Fig. 1. Finite-element model of a dual-layer gelatin gel.

dual-layer gel was assumed to be a deformable cylinder consisting of two perfectly bonded layers. The material properties of each layer were assumed to be isotropic and homogeneous and were described by a finite-strain hyperelastic neo-Hookean constitutive model [21]. The micropipette was assumed to be rigid and fixed with a smooth round edge at the pipette tip. The pipette tip fillet radius was 10% of the pipette inner diameter based on previous measurements [19]. The interaction between the gel and the micropipette was considered as a surface-based contact problem with the micropipette being modeled as a rigid surface in contact with the deformable gel surface. The displacement of the gel was constrained by the interaction between the gel top surface and micropipette. Traction-free finite sliding was allowed between the gel top surface and the micropipette surface. The applied load was modeled as a pressure boundary condition,  $\Delta P$ , over the free surface of the gel within the micropipette opening.

Owing to the axisymmetry of the problem, an eight-node second-order axisymmetric element with displacement–pressure hybrid formulation was chosen to discretize the dual-layer gel. The mesh was refined near the pipette opening to account for the high strain gradient in this region. Mesh convergence studies were performed to ensure the accuracy of the solution. The final model had approximately 1300 elements. The FE analysis was performed using ANSYS v. 11.0 (ANSYS Inc., Canonsburg, PA).

### 2.2. Parametric FE analysis of the dual-layer gel model

Here we define the elastic modulus of a dual-layer biomaterial measured by MA as the apparent elastic modulus ( $E_{app}$ ), and use the ratio of the apparent modulus to the modulus of the top layer ( $E_{top}$ ) to characterize the deviation of the measured modulus from the actual top layer modulus. The sensitivity of  $E_{app}/E_{top}$  to: (i) the ratio of the pipette diameter to the top layer thickness ( $D/t_{top}$ ); (ii) the ratio of the elastic modulus of the two layers ( $E_{top}/E_{bot}$ ); and (iii) the ratio of the pipette diameter to the bottom layer thickness ( $D/t_{bot}$ ) were evaluated, as these experimental parameters have been suggested to affect the measured elastic modulus of single-layer and multilayer biomaterials measured by MA [2,12,13]. The values of the parameters used were:  $D/t_{top}$  ratio = 0.2, 0.3, 0.5, 1.0, 1.5, 2.5, 4.0 and 5.0, with  $D/t_{bot}$  ratio  $\leq 0.5$  (equivalent to  $0.1 \leq t_{top}/t_{bot} \leq 2.5$ );  $E_{top}/E_{bot} = 0.333, 0.5, 0.625, 1.6, 2$  and 3; and  $D/t_{bot} = 0.2, 0.5, 1.0, 2.0$  and 5.0, with  $D/t_{top}$  ratio = 1.0 (equivalent to  $0.2 \leq t_{top}/t_{bot} \leq 5.0$ ). FE models of dual-layer gels with these parameters were created assuming a maximum applied pressure of  $\Delta P_{max}/E_{top} = 2.5$  and a pipette diameter of  $D = 0.93$  mm. Normalized load–deformation curves were generated by normalizing the applied pressure ( $\Delta P$ ) to the top layer elastic modulus ( $E_{top}$ ) and the aspiration length ( $L$ ) to the pipette radius ( $R = D/2$ ).

### 2.3. Inverse FE method to estimate gel elastic modulus

To obtain the apparent elastic moduli of the dual-layer gels modeled in the parametric FE study and gelatin gels tested in the MA experiment (Section 2.5), an inverse FE method was developed, similar to that described previously [19]. Briefly, the normalized load–deformation curves either predicted by the FE dual-layer gel models or measured from the gelatin gel MA experiment were used as “target” curves. The elastic modulus of a homogeneous gel model with the same overall thickness as either the dual-layer gel model or the gelatin gel was iteratively adjusted until its normalized load–deformation curve matched the target curve. The resulting elastic modulus was defined as the apparent elastic modulus of the dual-layer gel. This method was implemented using the Levenberg–Marquardt algorithm in a Matlab routine that was coupled with ANSYS [19].

#### 2.4. Dual-layer gelatin gel fabrication

Thirty per cent and ten per cent hydrated type B bovine gelatin (Sigma–Aldrich, Oakville, ON, Canada) gels were manufactured using sterile procedures, excluding gelatin powder sterilization (Fig. 2). Gelatin was dissolved in sterile double-distilled (dd) H<sub>2</sub>O at 60–65 °C for 15 min (30% gel) or 5 min (10% gel). Samples were maintained at 35 °C and dispensed into metal 37 × 24 × 5 mm<sup>3</sup> histology molds (Fisher Scientific, Ottawa, ON, Canada) at 32 °C. Layer 1 of the dual-layer constructs was dispensed into the mold on a 60 °C hotplate, and then cooled over ice (~15 °C) for 5 min/0.5 ml<sub>solution</sub>. Layer 2 was then added within the mold at room temperature, and then cooled over ice (~15 °C) for 5 min/0.5 ml<sub>solution</sub>. Gels were released from the mold and placed in sterile ddH<sub>2</sub>O, free floating on a shaker at room temperature for 2.5 days.

#### 2.5. MA of dual-layer gelatin gels

The apparent elastic moduli ( $E_{app}$ ) of hydrated dual-layer gelatin gels were determined experimentally by MA and normalized to the top layer elastic modulus ( $E_{top}$ ). To account for variability in gelatin composition and gel fabrication from batch to batch,  $E_{top}$  was determined by performing MA on homogeneous dual-layer gels in which both layers had the same material composition as the top layer for each gelatin batch. The bottom layer elastic modulus ( $E_{bot}$ ) was determined similarly for each batch on homogeneous dual-layer gels having the same material composition as the bottom layer. Based on these measurements, the  $E_{top}/E_{bot}$  ratios tested include 0.52, 0.66, 1.52 and 1.92, with various  $D/t_{top}$  ratios. These ratios were within the range tested in the parametric FE study.

The hydrated gels were maintained partially submerged in ddH<sub>2</sub>O (~20 min per spot tested), with rehydration for >1 h between spot tests. Pressure was applied against the top layer with a polished Pasteur pipette with ddH<sub>2</sub>O in the tip (1.03 or 1.018 mm inner diameter; outer diameter to inner diameter ratio of 2), controlled by a MX7630 micromanipulator (Siskiyou Corp., Grand Pass, OR, USA). Pressure was generated using a 20 ml air-filled syringe attached to a linear actuator (Ultra Motion, Cutchogue, NY, USA) with a step motor driver (Applied Motion Products, Watsonville, CA, USA) controlled by LabView (National Instruments, Austin, TX, USA), which applied 0.1 cm steps (~2 kPa) at 400 Hz to a maximum applied pressure of 6–16 kPa. Pressure was measured with a pressure sensor (30 PSI-D1-4V-MINI; All Sensors, Morgan Hill, CA, USA) and voltage meter. The deformation was imaged with an Olympus SZ61 stereoscope (Olympus,

Markham, ON, Canada) and a Canon Powershot digital camera (Canon Canada, Mississauga, ON, Canada) using PSRemote (Breeze Systems, Bagshot, Surrey, UK). Images were taken at equilibrium (5 min) after each pressure step. Two to five spots on each gel were tested. Aspiration lengths for each step were measured with ImageJ and normalized to the pipette radius. The apparent elastic moduli of the dual-layer gels ( $E_{app}$ ) and the elastic moduli of the homogeneous top ( $E_{top}$ ) and bottom ( $E_{bot}$ ) layer gels were estimated using the inverse FE method, as described in Section 2.3. To explicitly demonstrate the correlation between the experimental study and the FE study, a parametric FE study was performed using the same elastic modulus ratios as those in the experimental study and the results were compared with those of the experiment.

#### 2.6. Gelatin layer thickness measurement

To measure the thickness of the individual gel layers, samples were cooled to 4 °C and sliced through the analysis area. Layers were pulled apart manually (Fig. 2) and the layers in the analysis area were imaged using an Olympus SZ61 stereoscope (Olympus) and a Canon Powershot digital camera (Canon Canada) using PSRemote (Breeze Systems). Layer thicknesses were measured with ImageJ.

#### 2.7. MA of aortic heart valve leaflets

Five porcine aortic heart valves were harvested from hearts obtained from a local abattoir (Quality Meat Packers, Toronto, ON, Canada). Valves underwent  $-1\text{ }^{\circ}\text{C min}^{-1}$  freezing with 10% DMSO (Sigma–Aldrich), storage at  $-80\text{ }^{\circ}\text{C}$ , and thawing prior to testing. The local moduli of the fibrosa and ventricularis sides of one leaflet per valve were tested with MA. The leaflets were suspended loosely flat within a bath of PBS with Ca<sup>2+</sup> and Mg<sup>2+</sup>, with the local test area raised slightly above the surrounding tissue. The MA protocol was the same as that used to test the gelatin gels, with the following exceptions: (i) pipettes with internal diameters of 145 or 50–60 μm were used to apply local pressure within the individual layers of the fibrosa and ventricularis, respectively, to provide  $D/t_{top} < 1$  [3,22] (see also Section 3.3); (ii) pressure was applied using a 1 ml glass liquid-filled syringe, which applied 0.01–0.16 cm steps (~0.5–5 kPa) to a maximum applied pressure of 18–21 kPa; (iii) pressure was measured with a Sensotec Bidirectional FP2000 pressure transducer (Hoskin Scientific, Burlington, ON, Canada); (iv) a Navitar 12× lens (Navitar, Rochester, NY, USA) was used for imaging, with images taken immediately after step application. Multiple spots were tested per leaflet (fibrosa:  $n = 15\text{--}16$ ; ventricularis:  $n = 6\text{--}9$ ), only excluding the free edge and attachment regions of the leaflet from the measurement locations. Leaflets were processed for paraffin histology and stained with a modified Movat's stain (Electron Microscopy Sciences, Hatfield, PA, USA).

The effective moduli of the valve layers were estimated using the inverse FE method, but using a finite-strain hyperelastic exponential constitutive model that is appropriate for soft tissues, including heart valve [23]:

$$W = 0.5 \times C[\exp(\alpha(I_1 - 3))] - 1 \quad (1)$$

where  $W$  is the strain energy,  $C$  and  $\alpha$  are material constants, and  $I_1$  is the first strain invariant, defined as  $I_1 = \lambda_1^2 + \lambda_2^2 + \lambda_3^2$ , with  $\lambda_1$ ,  $\lambda_2$  and  $\lambda_3$  being the principal stretches. This isotropic exponential constitutive model was implemented numerically in ANSYS through the user material subroutine USERHYPER. The elastic properties of the region measured by MA were described by the product of the two material constants:

$$M = C\alpha \quad (2)$$

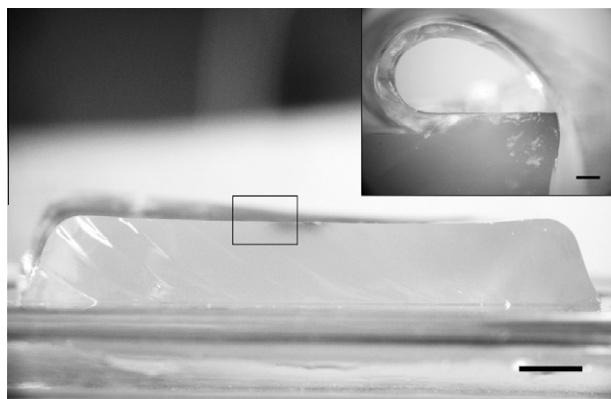


Fig. 2. Dual-layer gelatin sample prior to layer separation and after layer separation (inset). Note that the presence of two layers is not evident until the layers are pulled apart. Scale bars = 4 mm and 0.5 mm (inset).

Here, the product  $C\alpha$  was called the “effective modulus” ( $M$ ) for consistency with the literature [15]. This is a derived measure of stiffness, indicative of the local, homogenized elastic properties within the region tested by MA (in this case, a region within a single layer of the leaflet). This parameter is useful for comparing stiffness between samples, but is not physically meaningful, nor is it to be confused with elastic modulus or the effective elastic properties of multiple layers.

## 2.8. Statistics

The statistical analysis of valve data was conducted using a mixed model (proc mixed SAS 9.2) to assess the effect of leaflet layer on the effective modulus. Because multiple measurements were done within each leaflet, and therefore were not independent, the leaflet was incorporated into the model as a subject effect, which accounts for possible underlying similarity within leaflet measures, and was specified as a random variable. This model is very similar to, and can be interpreted as, a repeated-measures ANOVA where leaflet is the repeated subject. The difference in these two models is that the mixed model allowed for leaflet to be specified appropriately as a random variable.

## 3. Results

### 3.1. Experimental parameters determined by parametric FE analyses

Using parametric FE analyses, we first tested the sensitivity of the load–deformation curves to the diameter of the pipette relative to the thickness of the top layer being measured. Both when the top layer was stiffer ( $E_{\text{top}}/E_{\text{bot}} = 2$ ) and softer ( $E_{\text{top}}/E_{\text{bot}} = 0.5$ ) than the bottom layer, the normalized load–deformation curves converged to the exact result when  $D/t_{\text{top}} = 0.2$  (Fig. 3A and B). However, the differences were negligible when the  $D/t_{\text{top}}$  ratio was less than 1.

The apparent elastic moduli of the simulated dual-layer gel models were obtained by the inverse FE method and the sensitivity of the ratio of the apparent to actual top layer elastic modulus ( $E_{\text{app}}/E_{\text{top}}$ ) to the  $D/t_{\text{top}}$  ratio was determined for different elastic modulus ratio groups (Fig. 3C). Consistent with the load–deformation curves, as the  $D/t_{\text{top}}$  ratio approached 0.2, the  $E_{\text{app}}/E_{\text{top}}$  ratio approached 1 for all the elastic modulus ratio groups. The deviation of the  $E_{\text{app}}/E_{\text{top}}$  ratio from unity was only 1.4% when the  $D/t_{\text{top}}$  ratio was less than 1, indicating that relatively accurate measurement of top layer modulus is achievable with pipettes whose diameter is equal to or smaller than the thickness of the top layer. Between different elastic modulus ratio ( $E_{\text{top}}/E_{\text{bot}}$ ) groups, the  $E_{\text{app}}/E_{\text{top}}$  ratio diverged further from unity as the elastic modulus ratio diverged from 1. Thus, the greater the discrepancy in the moduli of the two layers, the greater the potential for erroneous measurement. It is also noteworthy that at large  $D/t_{\text{top}}$  ratios, the  $E_{\text{app}}/E_{\text{top}}$  ratio of the models with  $E_{\text{top}}/E_{\text{bot}}$  ratios less than 1 (soft top layer) diverged further from unity as compared with that of the models with  $E_{\text{top}}/E_{\text{bot}}$  ratios larger than 1 (stiff top layer). The apparent greater divergence with the soft top layer models is in part an artifact of the metric we used to assess accuracy of the measurement, but also suggests that measurement of soft top layers is more susceptible to the “stiffening effect” of the bottom layer when the pipette diameter exceeds the top layer thickness.

We also tested the sensitivity of the ratio of the apparent to actual top layer elastic modulus ( $E_{\text{app}}/E_{\text{top}}$ ) to the ratio of the pipette diameter to bottom layer thickness ( $D/t_{\text{bot}}$ ) for different elastic modulus ratio groups. While there was a small influence of  $D/t_{\text{bot}}$  on the apparent modulus, the deviation of the  $E_{\text{app}}/E_{\text{top}}$  ratio from unity was less than 2% for  $0.2 \leq D/t_{\text{bot}} \leq 5$  when  $D/t_{\text{top}}$  was 1

(Fig. 4). Thus, accurate measurement of top layer modulus requires  $D/t_{\text{top}} < 1$ , in which case the bottom layer thickness is essentially inconsequential.

### 3.2. Experimental validation using the gelatin system

To validate the FE model predictions experimentally, we made 27 MA measurements on nine dual-layer gelatin gels (Table 1). The dual-layer gels remained perfectly bonded during aspiration, as determined by visual and physical inspection and by the fact that MA of homogeneous single- and dual-layer gels yielded identical results (data not shown). The apparent elastic moduli  $E_{\text{app}}$  of both the dual-layer gels and homogeneous dual-layer gels were estimated using the inverse FE method. The fitting quality of the inverse FE method was excellent ( $R^2 > 0.99$ ).

The experimental trends agreed reasonably well with those predicted by the parametric FE analyses, although the measured apparent moduli tended to deviate slightly more from the actual top layer moduli than did those predicted by the FE (Fig. 5). Similar to the trend observed in the parametric FE study,  $E_{\text{app}}/E_{\text{top}}$  approached unity as the  $D/t_{\text{top}}$  ratio decreased (Table 1). Additionally, as predicted by the FE model, errors in the measured apparent moduli were more pronounced for soft top gels than stiff top gels for similar  $D/t_{\text{top}}$  ratios (Table 1 and Fig. 5).

### 3.3. Measurement of aortic valve layer-specific moduli

To demonstrate the utility of MA to measure the mechanical properties of individual layers in an intact tissue, we measured the effective elastic moduli of the fibrosa and ventricularis layers of porcine aortic heart valve leaflets. The fibrosa and ventricularis are layers on opposite sides of aortic valve leaflets, separated by a middle layer (the spongiosa). The three layers have distinct extracellular matrix composition [24], and based on tensile testing of dissected layers, the fibrosa is stiffer than the ventricularis [25]. However, the nonlinear mechanical properties of local regions of intact layers have not been measured. We did so using MA and pipettes with inner diameters less than the typical leaflet layer thicknesses (based on our own measurements and those reported in the literature [3,22]) to measure only a single layer. The thicknesses of MA test locations ( $n = 29$ ) were 197–491 and 78–205  $\mu\text{m}$  for the fibrosa and ventricularis, respectively, verifying that the pipette diameters used were the correct size for measurement of fibrosa or ventricularis properties only. Load–deformation curves were analyzed by the inverse FE method using a finite-strain hyperelastic exponential constitutive model (Fig. 6). Consistent with tensile test results [25], we found that the mean effective modulus of the fibrosa was greater than that of the ventricularis ( $P < 0.01$ ; Fig. 7). Of note, we observed considerable heterogeneity in the focal moduli within both layers, but with distinct stiff (effective moduli  $> 3$  kPa) and soft (effective moduli  $< 0.5$  kPa) regions in the fibrosa and ventricularis, respectively. These observations illustrate one advantage of a micromechanical test method such as MA over macroscale methods in which focal variations in mechanical properties are homogenized over sample dimensions of millimeters or greater.

## 4. Discussion

The simplicity and accessibility of MA have made it a relatively popular method to measure the bulk mechanical properties of cells, tissues and biomaterials [10–18]. However, its ability to measure the bulk properties of single layers in inhomogeneous multilayered biomaterials has not been fully investigated or confirmed experimentally. Here we used parametric nonlinear FE analyses,

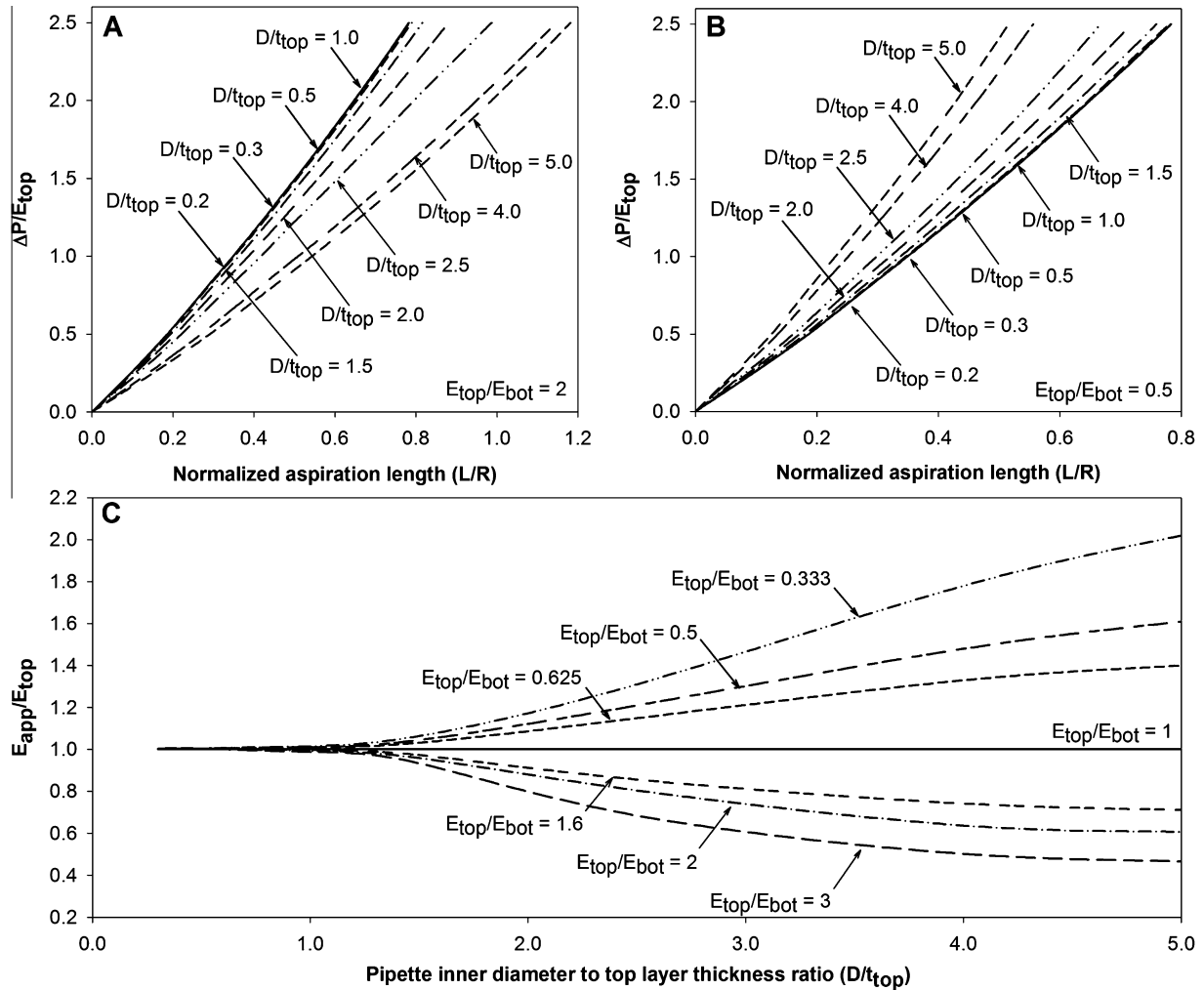


**Fig. 3.** (A) Normalized load–deformation curves for elastic modulus ratio group of  $E_{top}/E_{bot} = 2$ ; (B) normalized load–deformation curves for elastic modulus ratio group of  $E_{top}/E_{bot} = 0.5$ ; (C) normalized apparent elastic modulus vs.  $D/t_{top}$  ratio as determined by the parametric FE analyses.

an inverse FE method, and an experimental model system to determine the experimental parameters required to measure the elastic properties of the top layer of a multilayered material by MA. We found that accurate measurements of top layer moduli can be obtained by using a pipette with an inner diameter that is less than the thickness of the top layer ( $D/t_{top} < 1$ ), regardless of the moduli of the other layers or the thickness of the underlying layer(s). Using

this approach, we measured distinct effective moduli of the fibrosa and ventricularis layers on opposite sides of intact aortic heart valves, and showed that the fibrosa was significantly stiffer than the ventricularis, consistent with observations from tensile testing of individual, dissected layers [25].

Previous theoretical studies have tested the sensitivity of the MA-measured elastic properties of a substrate to its thickness for single- and dual-layer materials [2,12,13]. Our current study extends these studies in at least three significant ways. First, our parametric study was based on a finite strain nonlinear hyperelastic material model that better approximates the elastic aspiration

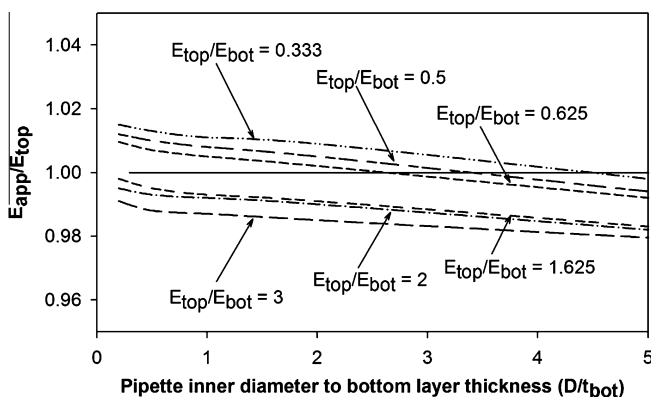


**Fig. 4.** Normalized apparent elastic modulus vs. the  $D/t_{bot}$  ratio as determined by the parametric FE analyses when  $D/t_{top} = 1$ .

**Table 1**

The sensitivity of the normalized apparent elastic modulus of dual-layer gelatin gels ( $E_{app}/E_{top}$ ) to the layer elastic modulus ratio ( $E_{top}/E_{bot}$ ) and the ratio of the pipette diameter to top layer thickness ( $D/t_{top}$ ).

Gel composition	$E_{top}/E_{bot}$	$D/t_{top}$	$E_{app}/E_{top}$ (mean $\pm$ SD)
10% Top/10% bottom	1.00	–	1.00 $\pm$ 0.04
10% Top/30% bottom	0.66	1.43	1.05 $\pm$ 0.04
	0.52	1.56	1.18 $\pm$ 0.05
	0.66	4.00	1.36 $\pm$ 0.06
30% Top/30% bottom	1.00	–	1.00 $\pm$ 0.06
30% Top/10% bottom	1.92	1.61	0.82 $\pm$ 0.02
	1.52	1.94	0.84 $\pm$ 0.03
	1.52	2.42	0.80 $\pm$ 0.04
	1.92	4.77	0.65 $\pm$ 0.02

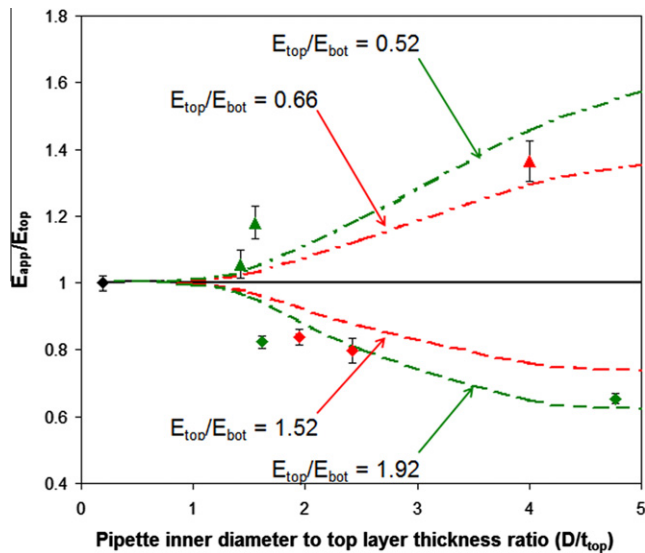


Fig. 5. Normalized apparent elastic modulus vs.  $D/t_{top}$  ratio as determined by the MA experiments of the dual-layer gelatin gels and predicted by the parametric FE analyses. Experimental data are presented as mean  $\pm$  standard deviation. Green, elastic modulus ratio groups of  $E_{top}/E_{bot} = 0.52$  (triangular) and 1.92 (circular); red, elastic modulus ratio groups of  $E_{top}/E_{bot} = 0.66$  (triangular) and 1.52 (circular).

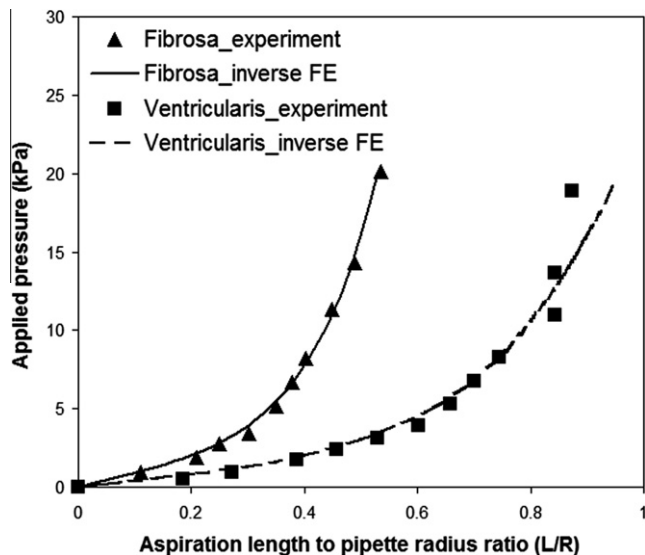


Fig. 6. The MA experimental load–deformation relationships of a typical fibrosa and ventricularis side of the aortic valve leaflet, and the nonlinear fitting curves determined by the inverse FE method based on the exponential constitutive model.

behavior of soft tissues and biomaterials than the linear elastic models used previously. Second, we implemented a versatile nonlinear inverse FE approach to analyze the experimental data. And third, we provided the first experimental validation of the FE predictions using a model dual-layer gelatin system.

Nonlinear analyses are important to interpret MA data, as the materials best suited for mechanical characterization by MA (i.e. soft tissues and biomaterials) typically have nonlinear stress–strain behaviors. Further, the large deformation that occurs in the protruded region of an aspirated material introduces geometric nonlinearities that are not captured by infinitesimal strain analyses. The result is nonlinear load–deformation behavior (Fig. 6), representing both material and geometric nonlinearities. While some previous studies have accounted for geometric nonlinearities, all assumed linear elastic material behavior [2,12,13]. Notably, Aoki

et al. [13] assumed linear elastic behavior of dual-layer substrates and predicted by FE analysis that  $D/t_{top} < 1$  was required to measure the elastic properties of only the top layer, consistent with our observations. Together, our study and that of Aoki et al. suggest that this critical value of  $D/t_{top}$  is independent of the substrate material constitutive behavior. We also showed here that measurement of the properties of the top layer is unaffected by the elastic properties and thickness of the underlying layer(s) if  $D/t_{top} < 1$ . Thus, an important and practical conclusion is that the  $D/t_{top} < 1$  criterion for pipette diameter selection can be applied universally and without knowledge of the substrate properties a priori.

Of course, selection of the appropriate pipette diameter to achieve  $D/t_{top} < 1$  requires knowledge of the top layer thickness. The top layer thickness will often be known or can be estimated, as is the case for the aortic valve. If it is unknown, then a pipette with as small a diameter as possible should be used, as we observed both numerically and experimentally that material parameter estimates improve as  $D/t_{top} \rightarrow 0$  (Fig. 5). The lower limit of the pipette diameter will be determined largely by the stiffness of the material relative to the maximum force that can be applied over the pipette opening and the ability to image the resulting aspiration lengths (the minimum measurable aspiration length was on the order of 1  $\mu\text{m}$  with the set-up used here). Alternatively, the thickness of the top layer could be estimated experimentally by testing with increasingly smaller diameter pipettes and identifying the diameter at which the measured apparent moduli converge.

Extraction of material parameters from MA data requires selection of a material model. While previous studies used linear elastic models, recent studies on MA of cells have shown that material parameter estimates are more accurate when nonlinear material behavior (typical of most soft tissues and biomaterials) is accounted for [19,26]. The inverse nonlinear FE approach developed here enables any material model to be implemented, thereby improving the MA method and broadening its applicability. We demonstrated this using a finite-strain hyperelastic exponential constitutive model to extract material parameters and effective moduli for the fibrosa and ventricularis layers of the aortic valve. Our observation that the fibrosa is significantly stiffer than the ventricularis agrees with results from previously reported micro-tensile tests [25], although direct comparison of the moduli is not possible because they reported incremental linear elastic moduli at a specific applied stress. By using MA, we were able to demonstrate for the first time significant heterogeneity in the local effective moduli of both layers of the aortic valve and that there are distinct regions in the fibrosa that are clearly stiffer than any in the ventricularis. Presumably focally stiff regions influence stress transfer to embedded valve interstitial cells (VICs) and resistance to cell-generated traction forces, which have been shown in vitro to regulate VIC phenotype [27–29].

A limitation of both the MA method and material models used here is that they are applicable only for isotropic, homogeneous materials. Due to the circumferential alignment of collagen fibers in the fibrosa and radial alignment in the ventricularis, both layers of the aortic valve exhibit significant anisotropic behavior [30] that we were not able to characterize in the current study. However, modifications to the MA method and the material model can be made to enable characterization of nonlinear, heterogeneous, anisotropic materials. For example, Ohashi et al. [18] used rectangular-shaped pipettes to measure the anisotropic properties of blood vessels by MA. Cox et al. [31,32] used microindentation and digital image correlation to track local deformations, and a fiber-reinforced composite material model to characterize the anisotropic properties of planar tissues; a similar approach could be adapted for use with MA. Additionally, viscoelastic behavior, also typical of many soft tissues and biomaterials, can be characterized by MA, as has been done with cells [19]. Each of

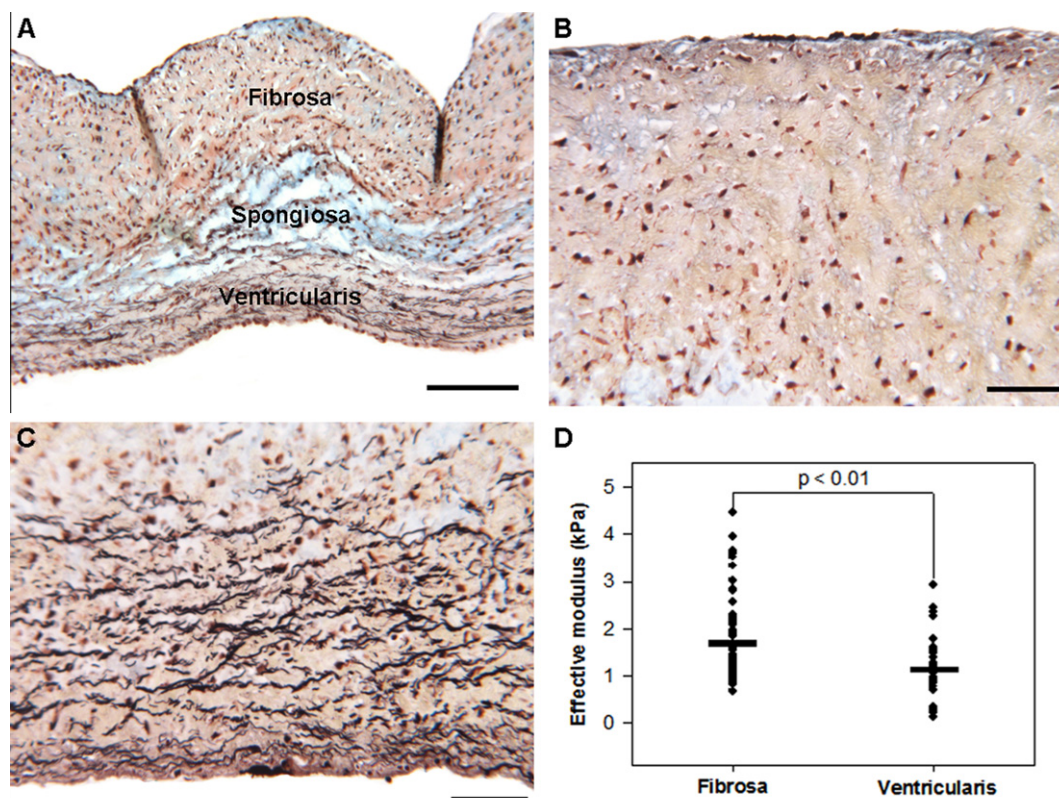


**Fig. 7.** (A) Aortic valve leaflet cross-section stained with modified Movat's pentachrome stain (scale = 150  $\mu\text{m}$ ). Representative MA test locations on the (B) fibrosa and (C) ventricularis marked with black dye (scale = 50  $\mu\text{m}$ ). (D) Effective moduli of the fibrosa and ventricularis sides of five aortic valve leaflets as determined by MA. (Number of spots tested: fibrosa = 71, ventricularis = 33).

these modifications would be facilitated by the inverse FE approach developed here.

## 5. Conclusions

The nonlinear elastic properties of the top layer of a multilayered material can be estimated by MA by using a pipette with a diameter smaller than the top layer thickness and an inverse FE method with an appropriate material model. This relatively simple and reliable method enables characterization of the local mechanical properties of a wide range of soft tissues and biomaterials.

## Acknowledgements

This study was supported by the Natural Science and Engineering Research Council of Canada (NSERC; RGPIN 327627-06), the Heart and Stroke Foundation (HSF) of Ontario (NA6047 and NA6654), an Ontario Early Researcher Award (to C.A.S.), HSF of Canada Doctoral Research Awards (to R.Z. and K.L.S.), an NSERC Canada Graduate Scholarship (to K.L.S.), and the Canada Research Chair in Mechanobiology (to C.A.S.).

## References

- [1] Diridollou S, Patat F, Gens F, Vaillant L, Black D, Lagarde JM, et al. In vivo model of the mechanical properties of the human skin under suction. *Skin Res Technol* 2000;6:214–21.
- [2] Alexopoulos LG, Haider MA, Vail TP, Guilak F. Alterations in the mechanical properties of the human chondrocyte pericellular matrix with osteoarthritis. *J Biomech Eng* 2003;125:323–33.
- [3] Stella JA, Sacks MS. On the biaxial mechanical properties of the layers of the aortic valve leaflet. *J Biomech Eng* 2007;129:757–66.
- [4] Fung YC, Liu SQ. Determination of the mechanical properties of the different layers of blood vessels in vivo. *Proc Natl Acad Sci USA* 1995;92:2169–73.
- [5] Dimitriadis EK, Horkay F, Maresca J, Kachar B, Chadwick RS. Determination of elastic moduli of thin layers of soft material using the atomic force microscope. *Biophys J* 2002;82:2798–810.
- [6] Boyer G, Zahouani H, Le Bot A, Laquieze L. In vivo characterization of viscoelastic properties of human skin using dynamic micro-indentation. *Conf Proc IEEE Eng Med Biol Soc* 2007;2007:4584–7.
- [7] Chaudhry B, Ashton H, Muhamed A, Yost M, Bull S, Frankel D. Nanoscale viscoelastic properties of an aligned collagen scaffold. *J Mater Sci Mater Med* 2009;20:257–63.
- [8] Gow BS, Castle WD, Legg MJ. An improved microindentation technique to measure changes in properties of arterial intima during atherosclerosis. *J Biomech* 1983;16:451–8.
- [9] Matsumoto T, Goto T, Furukawa T, Sato M. Residual stress and strain in the lamellar unit of the porcine aorta: experiment and analysis. *J Biomech* 2004;37:807–15.
- [10] Matsumoto T, Abe H, Ohashi T, Kato Y, Sato M. Local elastic modulus of atherosclerotic lesions of rabbit thoracic aortas measured by pipette aspiration method. *Physiol Meas* 2002;23:635–48.
- [11] Boudou T, Ohayon J, Picart C, Tracqui P. An extended relationship for the characterization of Young's modulus and Poisson's ratio of tunable polyacrylamide gels. *Biorheology* 2006;43:721–8.
- [12] Boudou T, Ohayon J, Arntz Y, Finet G, Picart C, Tracqui P. An extended modeling of the micropipette aspiration experiment for the characterization of the Young's modulus and Poisson's ratio of adherent thin biological samples: numerical and experimental studies. *J Biomech* 2006;39:1677–85.
- [13] Aoki T, Ohashi T, Matsumoto T, Sato M. The pipette aspiration applied to the local stiffness measurement of soft tissues. *Ann Biomed Eng* 1997;25:581–7.
- [14] Kauer M, Vuskovic V, Dual J, Szekely G, Bajka M. Inverse finite element characterization of soft tissues. *Med Image Anal* 2002;6:275–87.
- [15] Butcher JT, McQuinn TC, Sedmera D, Turner D, Markwald RR. Transitions in early embryonic atrioventricular valvular function correspond with changes in cushion biomechanics that are predictable by tissue composition. *Circ Res* 2007;100:1503–11.
- [16] Ozawa H, Matsumoto T, Ohashi T, Sato M, Kokubun S. Comparison of spinal cord gray matter and white matter softness: measurement by pipette aspiration method. *J Neurosurg* 2001;95:221–4.
- [17] Ohashi T, Kato Y, Matsumoto T, Sato M. Intramural distribution of elastic moduli in thoracic aortas and its relationship to histology: comparison between porcine and bovine thoracic aortas. *JSME Int J* 1999;42:568–73.

- [18] Ohashi T, Abe H, Matsumoto T, Sato M. Pipette aspiration technique for the measurement of nonlinear and anisotropic mechanical properties of blood vessel walls under biaxial stretch. *J Biomech* 2005;38:2248–56.
- [19] Zhao R, Wyss K, Simmons CA. Comparison of analytical and inverse finite element approaches to estimate cell viscoelastic properties by micropipette aspiration. *J Biomech* 2009;42:2768–73.
- [20] Holzapfel GA, Ogden RW. *Mechanics of biological tissue*. New York: Springer-Verlag; 2006.
- [21] ANSYS. ANSYS structural analysis guide (version 11.0). Canonsburg, PA: ANSYS Inc.; 2006.
- [22] Merryman WD, Huang HY, Schoen FJ, Sacks MS. The effects of cellular contraction on aortic valve leaflet flexural stiffness. *J Biomech* 2006;39:88–96.
- [23] Usyk TP, McCulloch A. In: Holzapfel GA, Ogden RW, editors. *Biomechanics of soft tissue in cardiovascular systems*. New York: Springer-Verlag; 2003. pp. 273–341.
- [24] Rabkin-Aikawa E, Farber M, Aikawa M, Schoen FJ. Dynamic and reversible changes of interstitial cell phenotype during remodeling of cardiac valves. *J Heart Valve Dis* 2004;13:841–7.
- [25] Vesely I, Noseworthy R. Micromechanics of the fibrosa and the ventricularis in aortic valve leaflets. *J Biomech* 1992;25:101–13.
- [26] Zhou EH, Lim CT, Quek ST. Finite element simulation of the micropipette aspiration of a living cell undergoing large viscoelastic deformation. *Mech Adv Mater Struct* 2005;12:12.
- [27] Pho M, Lee W, Watt DR, Laschinger C, Simmons CA, McCulloch CA. Cofilin is a marker of myofibroblast differentiation in cells from porcine aortic cardiac valves. *Am J Physiol Heart Circ Physiol* 2008;294:H1767–78.
- [28] Yip CY, Chen JH, Zhao R, Simmons CA. Calcification by valve interstitial cells is regulated by the stiffness of the extracellular matrix. *Arterioscler Thromb Vasc Biol* 2009;29:936–42.
- [29] Merryman WD, Lukoff HD, Long RA, Engelmayr Jr GC, Hopkins RA, Sacks MS. Synergistic effects of cyclic tension and transforming growth factor- $\beta$ 1 on the aortic valve myofibroblast. *Cardiovasc Pathol* 2007;16:268–76.
- [30] Sacks MS, David Merryman W, Schmidt DE. On the biomechanics of heart valve function. *J Biomech* 2009;42:1804–24.
- [31] Cox MA, Driessen NJ, Bouten CV, Baaijens FP. Mechanical characterization of anisotropic planar biological soft tissues using large indentation: a computational feasibility study. *J Biomech Eng* 2006;128:428–36.
- [32] Cox MA, Driessen NJ, Boerboom RA, Bouten CV, Baaijens FP. Mechanical characterization of anisotropic planar biological soft tissues using finite indentation: experimental feasibility. *J Biomech* 2008;41:422–9.